Electronic supplementary material

Resonant Amplification of Intrinsic Magnon Modes and Generation of New Extrinsic Modes in a Two-Dimensional Array of Interacting Multiferroic Nanomagnets by Surface Acoustic Waves

Anulekha De,[a] Justine Lynn Drobitch,[b] Sudip Majumder,[a] Saswati Barman,[c] Supriyo Bandyopadhyay,[c] and Anjan Barman[*a]

S1. NATURE OF THE SURFACE ACOUSTIC MODES

The surface acoustic wave (SAW) in this experiment is generated by applying a time-varying voltage between two electrodes delineated on a piezoelectric substrate. Hence, it is not a traditional Rayleigh, Sezawa, Lamb or Love mode which are usually launched with interdigitated transducers (IDTs). IDTs are not mandatory to generate surface acoustic waves since even Rayleigh mode SAW has been generated with coplanar electrodes in $LiNbO_3$ superlattices [1]. In our case we do not have a superlattice, but the time-varying potential difference between the two electrodes creates a time varying strain in the intervening piezoelectric material. The material between the electrodes is therefore expanding and contracting periodically. This time varying strain will always generate an acoustic wave (phonons).

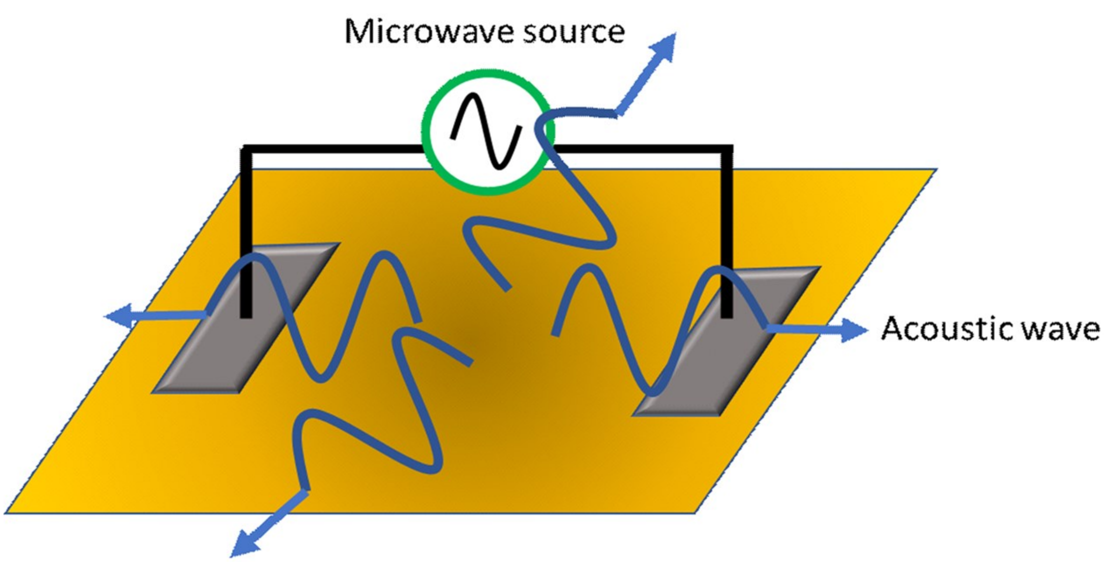

Figure S1: Surface acoustic waves generated by applying a time-varying potential between two electrodes delineated on a piezoelectric substrate.

In our case, this wave would be omni-directional as shown in Fig. S-1.

The longitudinal velocity of sound in a solid is $\sqrt{c_{11}/\rho}$ where c_{11} is the first diagonal element of the elasticity tensor and ρ is the mass density, while the shear velocity is $\sqrt{c_{44}/\rho}$. For $LiNbO_3$, c_{11} = 202 GPa, c_{44} = 50 GPa [2] and ρ = 4650 Kg/m^3. This results in a longitudinal sound velocity of 6.6 km/s and shear velocity of 3.3 km/s. Note that these are on the same order as the velocity of a Rayleigh wave in $LiNbO_3$, which is around 4 km/s. The velocity of the acoustic wave in our case is therefore also expected to be on this order. The wavelength of our acoustic wave in the frequency range of 1-10 GHz is then few hundred nm to few μm, whereas the separation between the electrodes is few mm. So, one can fit several wavelengths within the separation between the electrodes, which will cause periodically varying strain in the gap between the electrodes. Hence, we call it an "acoustic wave". The next question is whether this is a "surface" acoustic wave. Normally, the wave will decay exponentially into the substrate and the depth at which it decays to 1/*e* times the surface amplitude is about the wavelength. The substrate thickness is 0.5 mm and therefore the depth at which it decays to 1/*e* time the surface amplitude is less than one-tenth the substrate thickness. Hence, we think of it as a "surface" acoustic wave because it is confined near the surface. Since we use GHz frequency excitation, the frequency of the acoustic wave is also in the GHz range.

S2: TIME-RESOLVED REFLECTIVITY DATA FROM THE $LiNbO_3$ SUBSTRATE

The time-resolved reflectivity signal measured from the bare $LiNbO_3$ substrate is shown in Fig. S2(a) and the corresponding FFT power spectrum is shown in Fig. S2b. The data measured from the bare substrate reveals no clear oscillation exhibiting only a noisy FFT power spectrum. This is presumably due to the fact that the laser heating and cooling effect sets up noisy strain-field oscillations in the substrate and that is captured in the reflectivity data.

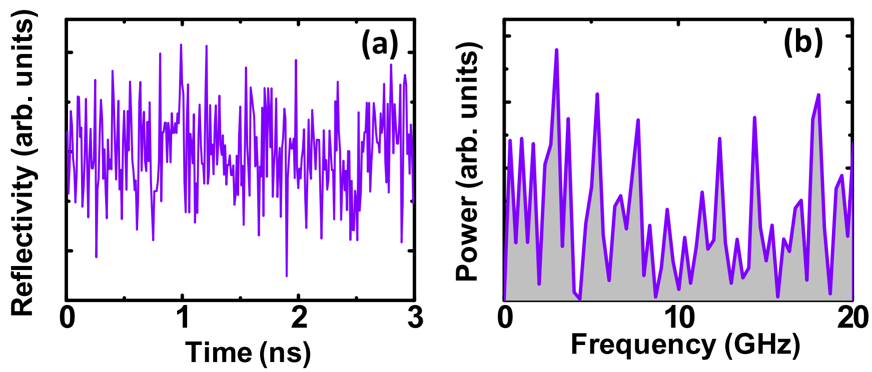

Figure S2: (a) Experimental time-resolved reflectivity data taken from the substrate and (b) the corresponding FFT power spectrum.

S3. MICROMAGNETIC SIMULATIONS OF SINGLE NANOMAGNET AT REMANENCE

We have simulated the magnetization dynamics of a single nanomagnet (with no dipole coupling with neighbors) to understand the SW dynamics within an isolated nanomagnet distinct from that of the array where inter-magnet dipole coupling plays a significant role. Figure S3(a) reveals that the ground state spin configuration of the single nanomagnet at remanence forms an '*S*' state. The fast Fourier transformed (FFT) power spectra of the simulated time-domain magnetization for the single nanomagnet as shown in Fig. S3(b) reveals four distinct SW modes at ~3.1 GHz (M1), ~4.1 GHz (M2), ~8.3 GHz (M3) and ~11.5 GHz (M4). Among them, the powers of modes M1 and M2 are much higher than those of the modes M3 and M4. The spatial profiles of the SW modes, calculated using the DOTMAG code [3], are shown in Fig. S3(c). It is evident that the modes M1 and M2 form standing wave patterns along the major axis of the ellipse, with quantization number n = 3. The mode M3 also forms a standing wave pattern in the same geometry with higher mode quantization number (n = 5). The highest frequency mode M4 forms a complex crisscross pattern with n = 7. It is noteworthy to mention that the spatial profiles of the SW modes are not symmetric. The axes of quantization of these modes are rotated due to the asymmetric '*S*' state spin configuration at remanence.

[a] *Department of Condensed Matter Physics and Material Sciences, S. N. Bose National Centre for Basic Sciences, Block JD, Sector-III, Salt Lake, Kolkata 700 106, India. Email: abarman@bose.res.in*
[b] *Department of Electrical and Computer Engineering, Virginia Commonwealth University, Richmond, VA 23284, USA.*
[c] *Institute of Engineering and Management, Sector V, Salt Lake, Kolkata, 700 091, India.*

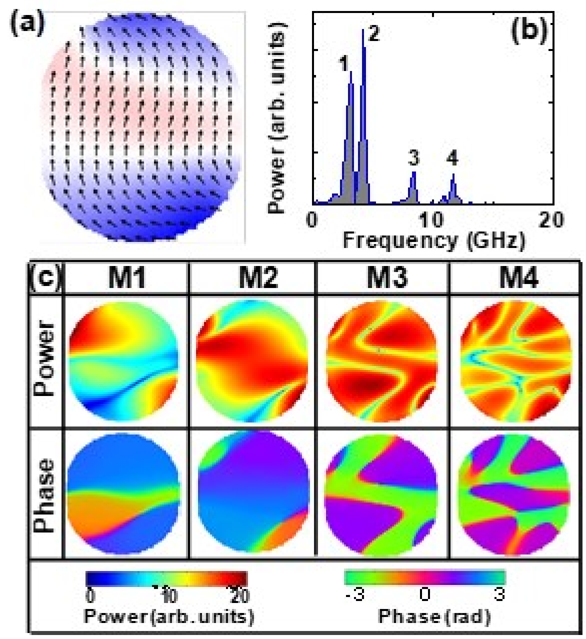

Figure S3: (a) Simulated ground state spin configuration within an isolated nanomagnet, (b) the FFT power spectra of the simulated time domain magnetization of the isolated nanomagnet, and (c) the power and phase profiles of the SW modes of the single isolated nanomagnet at remanence. The color bars are shown at the bottom.

S4: SPATIAL PROFILES OF THE INTRINSIC SW MODES (M1, M2 AND M4) AFTER APPLICATION OF SAW

The spatial profiles of the intrinsic SW modes (M1, M2 and M4) after application of SAW whose frequencies are in resonance with those of the modes are shown in Fig. S4. We have observed that the intrinsic SW modes, whose frequencies are resonant with the

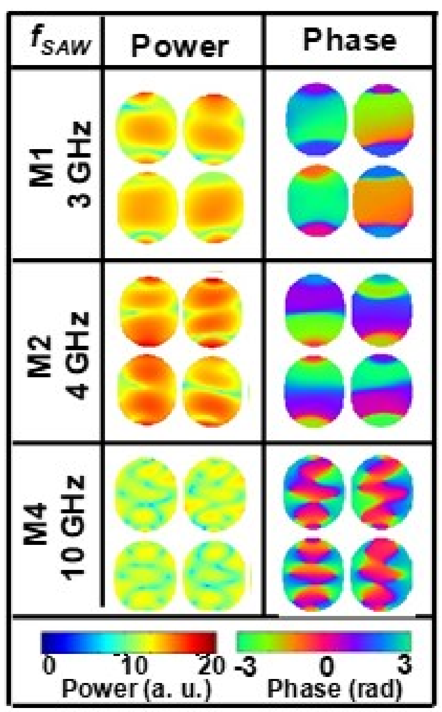

Figure S4: The power and phase profiles of the resonant SW modes at different values of f_{SAW}. The color bars are shown in the figure.

SAW frequencies, become more spatially uniform upon application of SAW. The modes M1 and M2 form standing wave patterns along the major axes with $n = 3$, and 4 respectively, whereas, the mode M4 has a complex characteristic with quantization occurring along both major ($n = 6$) and minor ($m = 3$) axis of the nanomagnet. The quantization numbers of M1 and M2 remain unaffected upon application of the SAW. However, for M4, the quantization along the minor axis changes after the application of SAW, while remaining unaffected along the major axis.

REFERENCES

1 D. Yudistrira, S. Benchabane, D. Janner and V. Pruneri, *Appl, Phys. Lett.,* 2009, **95**, 052901.

2 H. Ogi, Y. Kawasaki and M. Hirao*, J. Appl. Phys*., 2002, **92**, 2451

3 D. Kumar, O. Dmytriiev, S. Ponraj, A. Barman, *J. Phys. D: Appl. Phys.,* 2012, **45**, No. 015001.